Experiments on anisotropic radial viscous fingering

Jordi Ignés-Mullol and J. V. Maher
Department of Physics and Astronomy, University of Pittsburgh, Pittsburgh, Pennsylvania 15260
(Received 25 September 1995)

We observe dendritic patterns in fluid flow in an anisotropic Hele-Shaw cell and measure the tip shapes and trajectories of individual dendritic branches under conditions where the pattern growth appears to be dominated by surface tension anisotropy and also under conditions where kinetic effects appear dominant. In each case, the tip position depends on a power law in the time, but the exponent of this power law can vary significantly among flow realizations. Averaging many growth exponents α yields $\bar{\alpha} = 0.64 \pm 0.09$ in the surface tension dominated regime and $\bar{\alpha} = 0.66 \pm 0.09$ in the kinetic regime. Restricting the analysis to realizations when α is very close to 0.6 shows great regularity across pattern regimes in the coefficient of the temporal dependence of the tip trajectory.

PACS number(s): 68.10.−m, 47.20.Gv, 68.70.+w, 47.20.Hw

I. INTRODUCTION

The effect of anisotropy on pattern formation, particularly on viscous fingering, has been studied extensively [1–10]. The presence of the anisotropy, generally introduced experimentally as a perturbation in the uniformity of the cell gap, generates a rich variety of morphologies [1,2,7]. Transitions between morphologies have been studied and morphology phase diagrams have been measured [2,4]. The distinction between different morphologies is, however, mainly qualitative (one can clearly distinguish a faceted from a tip-splitting from a dendritic morphology). Still needed are quantitative ways to identify the morphology of a given pattern and, especially a quantitative way of describing the morphology phase transitions. The goal of the experiments reported herein was to obtain a quantitative signature of the morphologies and to exploit this to describe the transition between morphologies. We have studied the transition from dendritic to tip-splitting patterns as the strength of the anisotropy is tuned down, observing the effects of the anisotropy vanish as it is made weaker. We were motivated by work of Almgren et al. [9], who described a signature of the anisotropy in the fingering patterns (dendrites) in the form of a scaling of the tip position with time that was only possible in the presence of anisotropy. Their analysis introduced observable parameters that can be used for quantification of the effects of the anisotropy as we vary our experimental control parameters.

II. EXPERIMENTAL SETUP

Our apparatus consists of a radial Hele-Shaw cell, with a top glass plate 1 in. thick (to minimize plate flexing [11]) and 23 in. in diameter. Heavy paraffin oil acted as the more viscous fluid filling the gap space and dry nitrogen was injected through the center of the top plate to generate the patterns. The viscosity of heavy paraffin oil is $\mu = 1.6$ P and the oil air surface tension $\sigma = 35$ dyn/cm at 22 °C. To introduce anisotropy, a plate with a rectangular array of grooves etched on it was placed inside the gap, acting as the bottom plate. This etched plate was a large circuit board (25×50 cm^2) with its copper layer photochemically etched to produce the rectangular lattice pattern. The grooves were 0.2 mm wide, 0.4 mm center to center in one direction, and 0.8 mm center to center in the other direction, with a depth of 0.07 mm, thus forming rectangular islands of copper, 0.2×0.6 mm^2 in size, 0.07 mm in height, and 0.2 mm of spacing between neighboring edges. Spacers were used to keep the top and bottom plates at a uniform distance b, thus setting the cell gap. Measurements were made with gaps ranging from 0.11 to 1.0 mm. Dry nitrogen was injected at a constant volumentric injection rate, which translates into a constant areal injection rate Q if the bubble has a uniform thickness (close to the cell gap). The developing fingering patterns were observed with a charge coupled device video camera and taped on an enhanced S-VHS recorder. The images were then digitazed and analyzed with the assistance of image analysis software [12].

III. ANISOTROPIC FINGERING

A. Effect of the anisotropy

It is known [4] that in anisotropic viscous fingering different morphologies can be obtained and morphology phase transitions between them can be observed. If the anisotropy is introduced through a regular array of grooves (such as in the present experiments), then increases in the driving force (injection rate) lead to changes in steady-state pattern morphology that progress through faceted, surface tension dendrite, tip-splitting, and kinetic dendrite regimes. In particular, let us focus on the two dendritic morphologies: At *low velocities*, dendrites grow away from the etched grooves, presumably because of surface tension effects, that is, the most favorable configuration is the one that minimizes the cross sectional area of the interface and that occurs

away from the grooves. At *high velocities*, dendrites grow along grooves, presumably because of kinetic effects, that is, the most favorable configuration is the one that minimizes the impedance to the flow and that occurs along the grooves, where the gap is larger.

It is a known fact [7,13] (and our observations concur) that for dendritic patterns to appear, some anisotropy needs to be present. However, if the strength of this anisotropy is very low, regular growth based on tip splitting will dominate the shape of the patterns. In a theoretical analysis, the effect of the anisotropy is introduced in the pressure boundary condition as

$$P|_S = \gamma f(\theta)\kappa + \beta g(\theta) v_n, \tag{1}$$

where γ is the surface tension, β is a kinetic coefficient, θ is the local angle between the normal to the interface and the lattice, v_n is the local normal velocity, and κ is the local curvature. The term proportional to v_n should dominate at high speeds (kinetic dendrites) while the term proportional to the curvature should dominate at low velocities (surface tension dendrites). Given that $f(\theta)$ and $g(\theta)$ should reflect the symmetry of the lattice, it is customary to use expressions of the kind

$$f(\theta) = 1 - \epsilon\cos(m\theta), \tag{2}$$

$$g(\theta) = 1 - \chi\cos(m\theta + \delta), \tag{3}$$

where ϵ and χ are the anisotropy parameters, and they should quantify the effect of the lattice on the patterns, i.e., they should quantify the strength of the anisotropy. The phase shift δ allows for some competition between kinetic and static terms in the selection of the direction of growth (for instance, $\delta \sim 45°$ seems to be what we would infer from our experimental observations). We have observed that the morphology of the patterns can be altered by modification of $a = \Delta b/b$, the ratio between the depth of the grooves to the average cell gap; Q, the areal injection rate; and the length scale of the gap modulation, that is, the length scale of the etched lattice. In our case, the lattice being rectangular, we will have two such length scales, one corresponding to each side of the rectangles. For instance, we cannot observe any effect of the etching on the fingering patterns for $b > 1.0$ mm, that is, for $a < 0.07$. For a fixed gap, we can observe the effect of Q (see Fig. 1). Also on Fig. 1 we can see the influence of the length scale of the etching when, for a given Q and b, there is a different behavior along different sides of the rectangular islands of the etched plate. When the ratio $a = \Delta b/b$ between the depth of the grooves (Δb) and the average cell gap (b) is large enough, and beyond a certain injection rate, dendritic patterns appear. The underlying twofold symmetry of the lattice of grooves is reflected at much longer length scales in a twofold symmetry of the resulting fingering patterns.

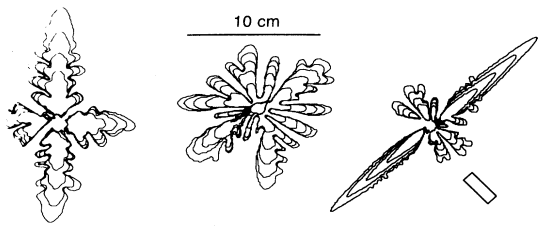

FIG. 1. For a gap $b = 0.11$ mm, dramatically different morphologies are observed. Left, $Q = 1.3$ cm^2/s generates surface-tension-controlled dendrites; center, $Q = 1.8$ cm^2/s generates a tip-splitting regime; right, $Q = 5.5$ cm^2/s generates a two-fold symmetric pattern with kinetic dendrites. The rectangle shows the orientation of the lattice.

B. Asymptotic scaling

Almgren *et al.* [9] studied the growth of fingering patterns in the presence of anisotropy by introducing an anistropy term in the pressure boundary condition

$$P|_S \sim \kappa[1 - \epsilon\cos(m\theta)]. \tag{4}$$

Thus they neglected kinetic effects completely. This is a simplification of the problem, but might appropriately be matched with the experiments at low driving force (assuming kinetic effects become small and possibly negligible). They predicted that, in the presence of anisotropy in the surface tension, the distance from the tip of a growing (surface-tension) dendrite to the injection point should scale with time as

$$x_{\text{tip}} = At^{3/5}. \tag{5}$$

If x is the coordinate along the axis of a growing dendrite and y is perpendicular to that axis, then, using simulation, they encounter a scaling behavior

$$x \sim t^{\alpha}, \tag{6}$$

$$y \sim t^{1-\alpha}, \tag{7}$$

where the fact that the exponents add up to one is a result of the constraint that the flow has constant injection rate (either areal or volumetric), so that the area of the pattern should grow linearly with time,

$$xy \sim t, \tag{8}$$

for any point inside a growing dendrite. This would be true if the flow is equally distributed among all dendrites (so that the individual area grows linearly with time and not only the total area of the multibranched bubble). This is automatically satisfied in the simulations, but is not always satisfied experimentally. They predicted that scaling behavior is asymptotic and experiments should observe it only after transients have relaxed. At each instant, the dendrite tip has the speed predicted by steady-state theory. Then, nondimensionalization yields the result that the steady-state tip should have a value for $\rho^2 V/d_0$ independent of time (it would be some function of the anisotropy parameter), where ρ is the tip radius of curvature, V is the tip velocity, and d_0 is the surface tension parameter. Considering the time-scaling assumption (5) and the constancy of $\rho^2 V$ one arrives at $\alpha = 3/5$. Almgren *et al.* are also able to find the asymptotic shape to which the time-rescaled dendrites

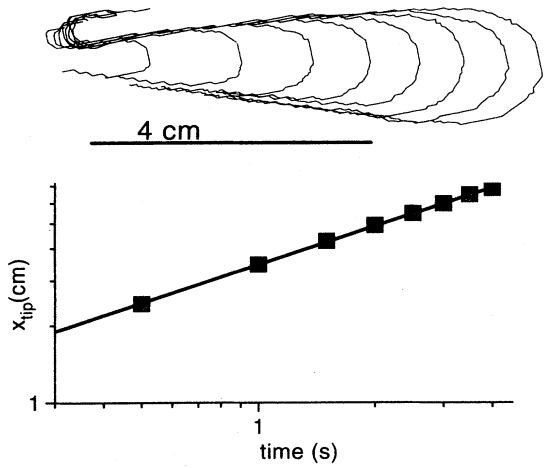

FIG. 2. Isotropic fingering (smooth plates) case. A finger that seems to suffer no competition effects, and before tip-splitting, displays a perfect $x_{tip} = At^{\alpha}$ scaling with $\alpha = 0.5$. It is, however, hard to find such an example because it will usually tip split or suffer strong competition before any sustained scaling regime is attained.

should converge. This curve has a dependence on the symmetry of the etching and is based on the finger being isolated (growing unperturbed by the other fingers). The exponent α, however, will be universal: the same for all kinds of anisotropy. Following the same arguments, it is easy to see that in the isotropic case (smooth plates), the only scaling should be with $\alpha = 0.5$ (the same for x and y axes) [8,11]. Moreover, one would need to obtain a finger that does not change topology (no tip splitting) and that does not feel a strong competition with the other fingers (its area should grow linearly with time) in order to observe such scaling (see Fig. 2).

IV. ANALYSIS OF THE EXPERIMENTAL DATA

To investigate the scaling behavior, we must obtain dendritic branches whose area grows linearly with time, that is, dendritic pieces of a larger pattern that are fed by a constant injection rate. Even though the analysis in [9] is restricted to surface-tension-controlled dendrites, we extend the analysis to kinetic-controlled dendrites as well. We have observed power-law behavior of the tip position in both regimes. Our analysis proceeds as follows. (i) For a dendrite in a given run, we examine succesive frames (up to 30 frames/s) and for each frame obtain its contour shape, from which we can measure the area and the tip position. This yields a time series for the area and the tip position. (ii) From the time series of the tip position, we obtain the time series for the distance from the tip to the injection point x_{tip} and try to fit to $x_{tip} = At^{\alpha}$. Sometimes, it is required to allow a small time shift t_0 to be fitted, due to a small uncertainty on the starting time for the flow, possibly including a transient time for the asymptotic flow to set up. We always require this time shift to be small, as compared to the time it takes the pattern to evolve. Also, we usually discard some of the first few frames, wherein shapes might be dominated by the transient. As noted above, the analysis in [9] predicts $\alpha = 3/5$ in the presence of anisotropy, for surface-tension dendrites. We have observed that values of α different from 3/5 fit our data better under a variety of conditions. It is plausible that the extension of the analysis to the kinetic regime may lead to other values for α.

For four-fold symmetry (case studied in [9]) the value of A as a function of ϵ has been computed analytically [14]. In our case, with two-fold symmetry and no reliable procedure to relate our experimental parameters with the anisotropy parameter ϵ that the theoretical treatment deals with, we must look for empirical regularity. With this parameter A and the value of Q both measured experimentally, we check whether our patterns conform to the universal asymptotic curves found in [9]. In general, there is a dispersion in the values of α, so patterns corresponding to the same morphology generate values of α that can be quite different. In the surface-tension-controlled regime, the analysis of 45 branches for several different gaps yields an average $\bar{\alpha} = 0.64$ with a large standard deviation $\sigma_{\alpha} = 0.098$. The analysis of 29 kinetic-controlled branches yields an average $\bar{\alpha} = 0.66$ with a standard deviation $\sigma_{\alpha} = 0.096$. Therefore, we can see no significant difference between the values of α in both regimes. A generalized trend is for the value of α to be larger than 0.5 (the one expected in the ab-

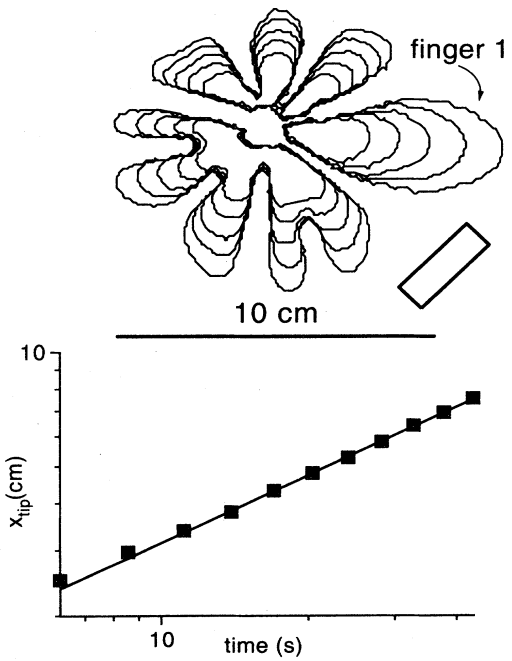

FIG. 3. Digitized patterns (top) and fit of tip position to t^{α} for the fastest growing branch (bottom) corresponding to a surface tension dendrite. That branch grows away from the grooves (at an angle of approximately 45°) and has a pointed tip (no tip splitting). The rectangle represents the orientation of the etching. The gap is $b \sim 0.3$ mm and the injection rate is $Q = 1.14$ cm^2/s. The t^{α} scaling behavior (with $\alpha = 0.59 \pm 0.07$ and $A = 0.80 \pm 0.02$) is observed after a short transient and no time shift parameter is required for the fit.

sence of anisotropy) and, in the case of surface-tension-controlled flow, consistent with the predicted value of 0.6. In Fig. 3 a run that generates a surface-tension dendrite is shown and the scaling exponent has a value in agreement with the expected 0.6. For this particular run, the rescaled shape does not conform with the asymptotic shapes found in [9], probably because of some interaction with the rest of the bubble, far behind the tip. The fact that the scaling of the tip position is so clear, however, can be interpreted as a sign that the selected velocity is only affected by what happens in the neighborhood of the tip and not on the full shape. Figure 4 shows a run in the kinetic-controlled regime, where dendritic branches follow the grooves. The dominant branch is analyzed and yields a value for α larger than 0.6. Using the value of Q for the whole bubble, we compare the rescaled data with the predicted asymptotic shape in the case of two-fold and four-fold symmetry. We notice that the two-fold shape adjusts better to our data

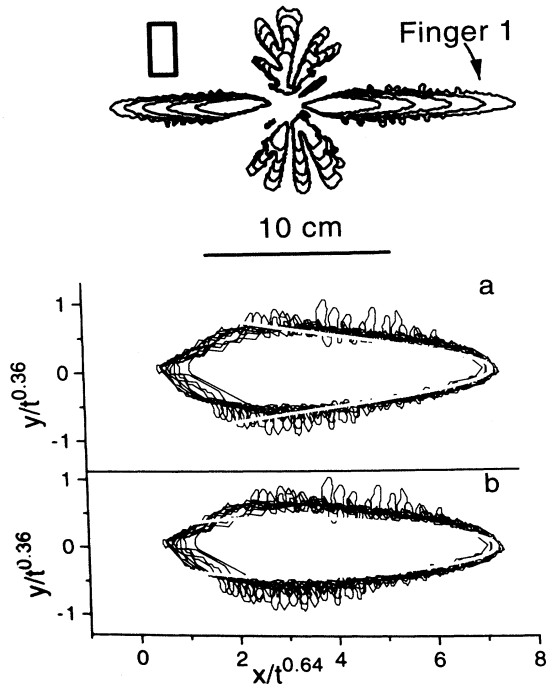

FIG. 4. Digitized patterns (top) and comparison of the rescaled shape with the predicted asymptotic curves for (a) twofold and (b) fourfold symmetry. The rectangle represents the orientation of the pattern. The gap is b=0.3 mm and the injection rate is $Q = 19.6$ cm^2/s. Note that while dendrites are observed along the short side of the rectangles, the long side still exhibits tip splitting. In the fit to the tip position, only the region where the area grows linearly with time has been used. This run coresponds to kinetic dendrites and the scaling of the tip position fits to the power law with $\alpha = 0.64 \pm 0.02$ and $A = 6.9 \pm 0.2$. A time offset of 0.3 s is required by this fit. Once A is found, the measured Q for the full pattern is used to scale the universal curve ($y/t^{1-\alpha} \sim \frac{Q}{A} y_{\text{universal}}$, $x/t^{\alpha} \sim A x_{\text{universal}}$). No other adjustments are made. Note that the rescaled empirical shapes at different times superimpose far behind the tips. The (a) two-fold asymptotic shape seems to adjust better than the (b) fourfold to these twofold data.

(see Fig. 4), which is what we would expect from having rectangular symmetry in the etching. Since the analysis that yields the theoretical expression for the asymptotic shapes relies on the symmetry of the problem, it may be reasonable that the same expressions could be used for surface-tension-controlled and for kinetic-controlled dendrites. Some preliminary arguments by Almgren [15] lead to the conclusion that a value $\alpha = 2/3$ is what should be found in the kinetic controlled regime, regardless of the symmetry of the anisotropy.

A. Quantitative analysis: Parameter A

Once convinced that our data were consistent with the predicted features of the anisotropic patterns, namely, the scaling as t^{α} of the tip position, we proceeded to study the evolution of A as the different experimental parameters that affect the patterns were varied. Our intention was to observe any available signature of a transition between the different morphologies or at least between anisotropic patterns and isotropic patterns. For each run, the pattern evolution of each of the dendrite branches obtained (up to 4 for high Q) was analyzed independently. The flow was not in general distributed uniformly among the different growing branches so the area of each branch within the same run would grow at a different rate. For this reason, we used the rate of growth of the area for each branch $\tilde{Q}$ as the relevant parameter instead of the global injection rate for the run. Doing this allowed us to obtain one independent value for A and one for α for each of the branches, up to four independent values for each flow realization. With this, we obtain a series of pairs (α, A) as a function of our control parameters $(b, \tilde{Q})$.

Most of the values for α we obtain are scattered around $\alpha = 0.6$. Our analysis concentrates on the dendrites that scale with $\alpha = 0.6$ (within experimental uncertainty; see the caption of Fig. 6 for more quantitative details). When we plot A vs $\tilde{Q}$, keeping the gap b fixed, we see the data align in a simple pattern that we can roughly describe with a power law: $A \sim \tilde{Q}^{\beta}$ (see Fig. 5). An even more striking result is that, if we put together in the same graph the data obtained from different gaps, they seem to superimpose, showing an apparent independence on the gap (see Fig. 6).

Karma has pointed out to us that the dependence of A on $\tilde{Q}$ at fixed b can be easily understood with some dimensional analysis [16] as follows: The equations of viscous flow in a radial Hele-Shaw cell can be made dimensionless by a suitable choice of units. Since the four-dimensional parameters of the experiment — Q, b, μ and σ — can be combined to produce the dimensionless quantity $\mu Q/\sigma b$, there is freedom in the way we nondimensionalize. A customary choice of units is $P_0 = \mu Q/b^2$ for pressure, $L_0 = b^2\sigma/(Q\mu)$ for length, and $T_0 = b^4\sigma^2/(\mu^2 Q^3)$ for time. Since μ (viscosity) and σ (surface tension) remain unchanged, we just need to focus on the dependence on Q and b. The above mentioned choice of units, namely, $P_0 \sim Q$, $L_0 \sim Q^{-1}$, and $T_0 \sim Q^{-3}$, effectively removes

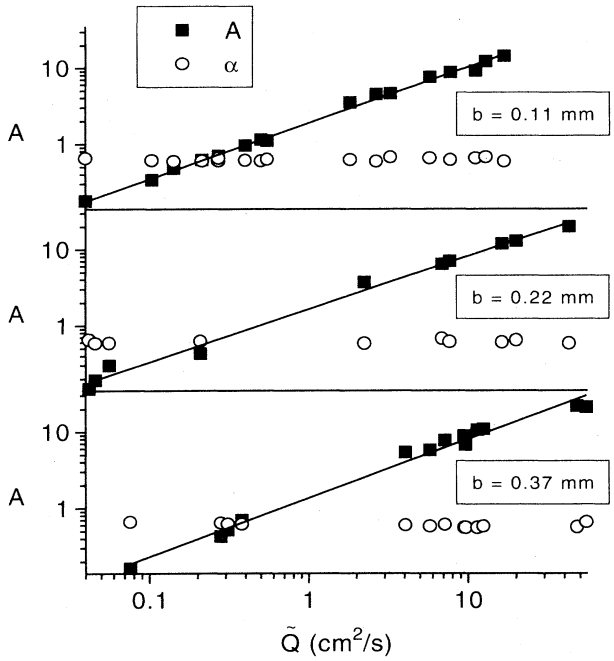

FIG. 5. Dependence of A (solid squares) on $\tilde{Q}$ for $\alpha \sim 0.6$ at three different values of the gap b. No distinction has been made between surface tension and kinetic dendrites, so branches from both regimes are present on the same graph. Note a regime of $\tilde{Q}$ values where there are no data. That regime connects surface tension dendrites (low $\tilde{Q}$) with kinetic dendrites (high $\tilde{Q}$) and there tip-splitting dominates the dynamics. The exponent of the power law is the following: top, $\beta = 0.74 \pm 0.01$; middle, $\beta = 0.70 \pm 0.02$; bottom, $\beta = 0.77 \pm 0.03$; open circles are the values of α for each case. The analysis presented in the text predicts a value $\beta = 0.8$.

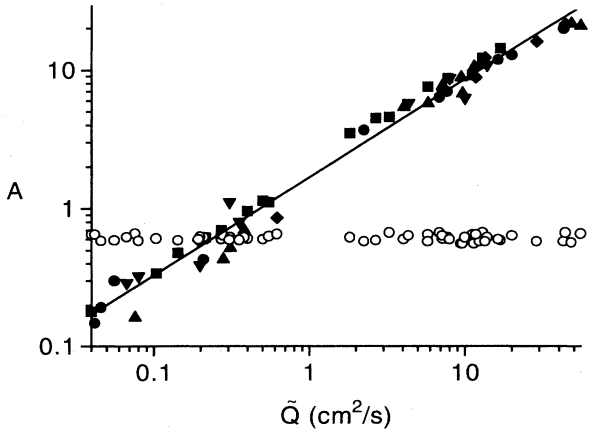

FIG. 6. A (solid symbols) vs $\tilde{Q}$ with $\alpha \sim 0.6$. The open circles are the values of α for each case. The two groups of data points correspond to surface tension dendrites (low $\tilde{Q}$) and kinetic dendrites (high $\tilde{Q}$). Gaps range from $b = 0.011$ cm up to $b = 0.037$ cm. In the surface tension regime $\bar{\alpha} = 0.62 \pm 0.02$ (24 points) and in the kinetic regime $\bar{\alpha} = 0.61 \pm 0.04$ (32 points). The combined statistics are $\bar{\alpha} = 0.61 \pm 0.03$ (56 points). The fit to a power law yields an exponent $\beta = 0.71 \pm 0.01$.

all dependence on Q from the equations. With this, the dimensionless pressure (p'), time (t'), and tip position (x') are expressed: $x \sim x'/Q$, $t \sim t'/Q^3$, and $p \sim Qp'$. Then, if we assume a scaling behavior $x' \sim A't'^{\alpha}$ (now A' is independent of Q, since Q is no longer present in the equations), the dimensional variables will verify

$$x \sim x'/Q \sim A't'^{\alpha}/Q \sim A'(tQ^3)^{\alpha}/Q = A'Q^{3\alpha-1}t^{\alpha}. \quad (9)$$

Now, if $\alpha \sim 0.6$ then we expect $A \sim \tilde{Q}^{0.8}$. Even though the above expressions have been derived using Q, the total injection rate, it is not unreasonable that, if a branch grows independently of the rest, being fed by a constant $\tilde{Q}$, the same expressions should hold with $\tilde{Q}$ instead of Q. That is what we check experimentally. This power-law behavior can be used as a proof for the self-consistency of the scaling of the tip position with time because it relies on two parameters (A and $\tilde{Q}$) that are measured by two experimentally independent methods.

Even though we found experimentally the surprising result that we can mix data from different gaps and yet obtain the same behavior (see Fig. 6), we can explore what dependence would A have on b by including b in the former analysis. If we include b, then the characteristic units of the problem go as $P_0 \sim Q/b^2$, $L_0 \sim b^2/Q$, and $T_0 \sim b^4/Q^3$. Once more, assuming $x' \sim A't'^{\alpha}$ we will have

$$x = x'L_0 \sim L_0 A' \left(\frac{tQ^3}{b^4}\right)^{\alpha} \sim A'\frac{b^2}{Q}t^{\alpha}Q^{3\alpha}b^{-4\alpha}$$
$$= A'Q^{3\alpha-1}b^{2(1-2\alpha)}t^{\alpha}. \quad (10)$$

So the expected behavior is $A \sim A'Q^{3\alpha-1}b^{2(1-2\alpha)}$. If $\alpha \sim 0.6$ this becomes $A \sim A'Q^{0.8}b^{-0.4}$ or, in a more compact way,

$$A \sim A'\left(\frac{Q}{\sqrt{b}}\right)^{0.8}.$$

Again, this should hold with $\tilde{Q}$ instead of Q for an individual branch. This has been tested on Fig. 7. We

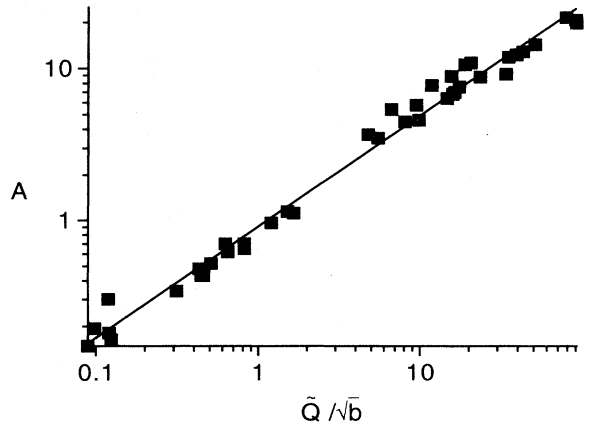

FIG. 7. A vs $\tilde{Q}/\sqrt{b}$ for $b = 0.11$ mm, $b = 0.22$ mm, and $b = 0.37$ mm combined. The fit to a power law yields an exponent $\beta = 0.73 \pm 0.01$.

see how in the range of b we used (from 0.011 cm up to 0.037 cm) the final result is not very much affected by the introduction of this dependence on b, even though we believe this last expression allows us to more confidently compare results obtained with different cell gaps.

V. SUMMARY AND CONCLUSIONS

Our experiments exhibit an asymptotic scaling of the tip position of a growing dendrite in viscous fingering in the presence of anisotropy. We have observed this scaling in both surface-tension-controlled and kinetic-controlled dendrites. Our analysis has independently extracted three parameters from our experimental data: A, the prefactor in the scaling of the tip position; $\tilde{Q}$, the rate of growth of the area of the dendrite branch; and α, the time exponent of the dendrite tip growth. While the theoretical results predict a single value of $\alpha = 0.6$ in the presence of static anisotropy and our individual measurements are frequently compatible with this value, we observe significant dispersion among the exponents observed in repeated flow realizations, yielding an averaged value of $\bar{\alpha} = 0.64 \pm 0.09$. For kinetic dendrites, $\bar{\alpha} = 0.66 \pm 0.09$. When we restrict our analysis to the flow realizations where $\alpha = 0.6$ ($\bar{\alpha} = 0.61 \pm 0.03$), we experimentally recover the relationship between A and $\tilde{Q}$ that the scaling of the tip position would impose (9) and (10). Thus far, the relatively large dispersion of α under conditions where the pattern was of unambiguous morphology has prevented us from meaningful comment on the quantification of the data in the morphology transition zones.

ACKNOWLEDGMENTS

We greatly appreciate many helpful comments and suggestions from David Jasnow, R. Almgren, and A. Karma. This work was supported by U.S. Department of Energy under Grant No. DE-FG02-84ER45131.

[1] E. Ben-Jacob *et al.*, Phys. Rev. Lett. **55**, 1315 (1985).
[2] V. Horvath, T. Vicsek, and J. Kertesz, Phys. Rev. A **35**, 2353 (1987).
[3] J. D. Chen, Exp. Fluids **5**, 363 (1987).
[4] E. Ben-Jacob, P. Garik, T. Mueller, and D. Grier, Phys. Rev. A **38**, 1370 (1988).
[5] D. A. Kessler, J. Koplik, and H. Levine, Adv. Phys. **37**, 255 (1988).
[6] S. K. Sarkar and D. Jasnow, Phys. Rev. A **39**, 5299 (1989).
[7] E. Ben-Jacob and P. Garik, Nature **343**, 523 (1990).
[8] M. Ben Amar, V. Hakim, M. Mashaal, and Y. Couder, Phys. Fluids A **3**, 1687 (1991).
[9] R. Almgren, W.-S. Dai, and V. Hakim, Phys. Rev. Lett. **71**, 3461 (1993).
[10] K. V. McCloud and J. V. Maher, Phys. Rev. E **51**, 1184 (1995).
[11] H. Thome, M. Rabaud, V. Hakim, and Y. Couder, Phys. Fluids A **1**, 224 (1989).
[12] BioScan Inc., Edmonds, WA, BIOSCAN OPTIMAS Version 3.01.
[13] E. Ben-Jacob, N. Goldenfeld, J. S. Langer, and G. Schon, Phys. Rev. Lett. **51**, 1930 (1983).
[14] M. Ben Amar and Y. Pomeau, Europhys. Lett. **2**, 307 (1986).
[15] R. Almgren (private communication).
[16] A. Karma (private communication).